



Preparation, crystal structure, thermal decomposition mechanism, and thermodynamical properties of $\text{H}[\text{Pr}(\text{NTO})_4(\text{H}_2\text{O})_4] \cdot 2\text{H}_2\text{O}^1$

Song Jirong^{a,*}, Hu Rongzu^b, Kang Bing^b, Li Fuping^b

^aDepartment of Chemical Engineering, Northwest University, Xi'an 710069, Shaanxi, China

^bXi'an Modern Chemistry Research Institute, Xi'an 710065, Shaanxi, China

Received 4 January 1999; accepted 17 May 1999

Abstract

$\text{H}[\text{Pr}(\text{NTO})_4(\text{H}_2\text{O})_4] \cdot 2\text{H}_2\text{O}$ was prepared by mixing the aqueous solution of lithium 3-nitro-1,2,4-triazol-5-onate and the dilute nitric acid solution of Pr_6O_{11} . The single crystal structure has been determined by a four-circle X-ray diffractometer. The crystal is triclinic, space group $\overline{\text{P}1}$ with crystal parameters of $a=1.0463(10)$ nm, $b=1.0484(10)$ nm, $c=1.1474(10)$ nm, $\alpha=99.10(10)^\circ$, $\beta=96.96(10)^\circ$, $\gamma=97.65(10)^\circ$, $V=1.2186(2)$ nm³, $Z=2$, $D_c=2.088$ g·cm⁻³, $\mu=21.17$ cm⁻¹, $F(0\ 0\ 0)=540$. The final R is 0.0206. Based on the thermal analysis, the thermal decomposition mechanism of $\text{H}[\text{Pr}(\text{NTO})_4(\text{H}_2\text{O})_4] \cdot 2\text{H}_2\text{O}$ has been derived. From measurements of the enthalpy of solution in water of $\text{H}[\text{Pr}(\text{NTO})_4(\text{H}_2\text{O})_4] \cdot 2\text{H}_2\text{O}$ at 298.15 K, the standard enthalpy of formation, lattice energy and lattice enthalpy have been determined as $-(2884.1 \pm 8.9)$, -5443.25 and -5473.25 kJ mol⁻¹, respectively. © 1999 Elsevier Science B.V. All rights reserved.

Keywords: Crystal structure; Praseodymium coordination; Enthalpy of solution; Lattice energy; Lattice enthalpy; NTO salt; Preparation; Standard enthalpy of formation; Thermal decomposition mechanism

1. Introduction

Much attention has been paid to 3-nitro-1,2,4-triazol-5-one (NTO) as a high energy and low sensitivity energetic material [1,2]. Its metal salts also have some potential uses in ammunition, propellant and energetic catalyst, especially its rare-earth metal salts [3–6]. Therefore the authors prepared the single crystal of $\text{H}[\text{Pr}(\text{NTO})_4(\text{H}_2\text{O})_4] \cdot 2\text{H}_2\text{O}$, measured its structure and

studied its thermal decomposition mechanism and thermodynamic properties.

2. Experimental

2.1. Materials

$\text{H}[\text{Pr}(\text{NTO})_4(\text{H}_2\text{O})_4] \cdot 2\text{H}_2\text{O}$ used in this research work was prepared according to the following method: an appropriate amount of Pr_6O_{11} was put into the dilute nitric acid solution and added the several milliliter of H_2O_2 . Stirred and titrated with an aqueous solution of lithium hydroxide under 60°C until pH reached 6–7, then with an aqueous solution of Li

*Corresponding author.

¹Presented at the Ninth Chinese Conference on Chemical Thermodynamics and Thermal Analysis (CTTA), Beijing, China, August 1998.

NTO·2H₂O and stirred at 60°C for 30 min. This solution was allowed to stand for about 12 h until a green precipitate formed. The precipitate was recrystallized with distilled water at room temperature to obtain the green single crystal for X-ray measurement. Its purity was more than 99.6%. Dimensions of the single crystal were 0.46×0.34×0.24 mm³. The conductivity of deionized water used in the experiment was 5.48×10⁻⁸ S cm⁻¹.

2.2. Experimental equipment and conditions

In the determination of the structure of the single crystal, X-ray intensities were recorded by a Siemens P₄ automatic diffractometer with graphite-monochromatized MoK_α radiation, $\lambda=0.071073$ nm. The 6479 independent reflections were obtained in the range of $3^\circ \leq 2\theta \leq 57^\circ$, among which 5650 with $F_0 > 4\sigma(F_0)$ were used for the determination and refinement of crystal structure. The crystal structure was obtained by direct method and every one of hydrogen atoms, except the hydrogen atoms of O(17) and O(18), by difference Fourier synthesis.

The thermal decomposition process was studied using a TG technique on a TGA-DTA instrument (TA, USA). The conditions of TG were as follows: sample mass, about 1 mg; heating rate, 10°C min⁻¹; atmosphere, static air. The DSC experiments were carried out with a model CDR-1 differential scanning calorimeter with a cell of aluminium (diameter 5 mm×3 mm) whose side was rolled up. The conditions of DSC were as follows: sample mass, about 1 mg; heating rate, 10°C min⁻¹; atmosphere, static air; reference sample, α-Al₂O₃; thermocouple plate, Ni/Cr–Ni/Si. The infrared spectra of the decomposition residues were recorded in KBr discs on a 60 SXR FT-IR spectrometer (Nicolet, USA) at 4 cm⁻¹ resolution.

All measurements of the enthalpy of solution in deionized water were made using a Calvet microcalorimeter, type BT215 from Setaram, France and operated at 298.15±0.01 K.

The experimental precision and accuracy of enthalpies of solution were frequently checked by measurement of the enthalpies of solution ($\Delta_{\text{sol}}H_{\infty}^0$) of crystalline KCl in deionized water at 298.15 K. The experimental value of $\Delta_{\text{sol}}H_{\infty}^0=(17.217\pm 0.053)$ kJ mol⁻¹ is in excellent agreement with that of

$\Delta_{\text{sol}}H_{\infty}^0=17.234$ kJ mol⁻¹ reported in the literature [7].

3. Results and discussion

3.1. Crystal structure

The crystal structure was found to be triclinic, which belongs to space group P $\overline{1}$ with crystallographic parameters of $a=1.0463(10)$ nm, $b=1.0484(10)$ nm, $c=1.1474(10)$ nm, $\alpha=99.10(10)^\circ$, $\beta=96.96(10)^\circ$, $\gamma=97.65(10)^\circ$, $V=1.2186(2)$ nm³, $Z=2$, $D_c=2.088$ g·cm⁻³, $\mu=21.17$ cm⁻¹, $F(0\ 0\ 0)=540$. The final $R=0.0206$ and $WR=0.0587$.

The atom coordinates, thermal parameters, bond lengths and bond angles are summarized in Tables 1–3. The molecular structure and atom labeling are shown in Fig. 1, the packing of the molecule in the crystal lattice and the coordination polyhedron of Pr³⁺ are illustrated in Figs. 2 and 3.

The analytical results indicate that the Pr atom, the four carbonyl oxygen of the four NTO cycles and four water molecules form [Pr(NTO)₄(H₂O)₄]⁻ which was a trigonal dodecahedron. By combining it with the hydrogen ion, H[Pr(NTO)₄(H₂O)₄] was obtained. There are two water molecules of crystallization in the crystal, denoted as H[Pr(NTO)₄(H₂O)₄]·2H₂O.

As shown in Table 2, the distance between Pr and the carbonyl oxygen of NTO cycle is 0.2378–0.2457 nm, between Pr and the coordination water is 0.2499–0.2608 nm. Because of the induction effect of Pr³⁺, the conjugate π-electrons of carbonyl oxygen O(1), O(4), O(7) and O(10) are partly shared between Pr–O(1), Pr–O(4), Pr–O(7) and Pr–O(10) and the coordination bonds become shorter.

According to the calculation, the equations of the planes of four NTO rings are as follows:

$$-6.214x - 6.615y + 6.376z = -5.0642 \quad (\text{I})$$

$$7.519x + 5.131y - 6.311z = 2.3456 \quad (\text{II})$$

$$7.909x + 4.743y - 6.015z = 1.5037 \quad (\text{III})$$

$$8.027x + 4.923y - 5.376z = 2.6338 \quad (\text{IV})$$

The dihedral angles between planes (I) and (II), (I) and (III), (II) and (III), (I) and (IV), (II) and (IV), (III)

Table 1
Positional parameters and U_{eq} ($\times 10^3$, in nm 2)

| Atom | <i>x</i> | <i>y</i> | <i>z</i> | U_{eq} |
|--------|-------------|------------|-------------|-----------------|
| Pr | -0.5729(1) | 0.9307(1) | -0.2622(1) | 0.18(1) |
| O(1) | -0.3574(2) | 0.9509(2) | -0.1539(2) | 0.33(1) |
| O(2) | 0.0711(3) | 0.7584(3) | 0.0581(2) | 0.60(1) |
| O(3) | 0.0049(2) | 0.9167(2) | 0.1685(2) | 0.43(1) |
| O(4) | -0.5799(2) | 1.1339(2) | -0.1359(2) | 0.34(1) |
| O(5) | -0.5848(2) | 1.5323(2) | 0.1750(2) | 0.42(1) |
| O(6) | -0.7316(3) | 1.6034(3) | 0.0650(2) | 0.68(1) |
| O(7) | -0.7093(2) | 0.9662(2) | -0.4317(2) | 0.34(1) |
| O(8) | -0.9251(3) | 1.3707(2) | -0.3712(2) | 0.58(1) |
| O(9) | -1.0166(3) | 1.3382(3) | -0.5547(2) | 0.59(1) |
| O(10) | -0.4841(2) | 0.8281(2) | -0.4360(2) | 0.29(1) |
| O(11) | -0.2641(2) | 0.3685(2) | -0.5144(3) | 0.55(1) |
| O(12) | -0.1966(3) | 0.4962(3) | -0.3452(2) | 0.55(1) |
| O(13) | -0.8155(2) | 0.8962(2) | -0.2261(2) | 0.35(1) |
| O(14) | -0.4453(2) | 1.1080(2) | -0.3419(2) | 0.32(1) |
| O(15) | -0.5775(2) | 0.6936(2) | -0.2350(2) | 0.35(1) |
| O(16) | -0.6149(2) | 0.8773(2) | -0.0576(2) | 0.32(1) |
| O(17) | 0.1917(2) | 0.7724(2) | 0.2941(2) | 0.44(1) |
| O(18) | 0.1166(3) | 0.6199(3) | 0.8124(2) | 0.61(1) |
| N(1) | -0.2203(2) | 0.7949(2) | -0.1815(2) | 0.28(1) |
| N(2) | -0.1171(2) | 0.7579(2) | -0.1188(2) | 0.31(1) |
| N(3) | -0.1832(2) | 0.9335(2) | -0.0114(2) | 0.25(1) |
| N(4) | 0.0022(2) | 0.8400(2) | 0.0754(2) | 0.34(1) |
| N(5) | -0.7112(2) | 1.2900(2) | -0.1726(2) | 0.29(1) |
| N(6) | -0.7388(2) | 1.4040(2) | -0.1121(2) | 0.31(1) |
| N(7) | -0.5867(2) | 1.3216(2) | 0.0022(2) | 0.25(1) |
| N(8) | -0.6595(2) | 1.5246(2) | 0.0830(2) | 0.34(1) |
| N(9) | -0.8613(2) | 1.0108(2) | -0.5784(2) | 0.28(1) |
| N(10) | -0.9356(2) | 1.1058(2) | -0.5951(2) | 0.29(1) |
| N(11) | -0.8120(2) | 1.1539(2) | -0.4114(2) | 0.26(1) |
| N(12) | -0.9519(2) | 1.3065(2) | -0.4717(2) | 0.36(1) |
| N(13) | -0.4590(2) | 0.6559(2) | -0.5830(2) | 0.25(1) |
| N(14) | -0.3942(2) | 0.5507(2) | -0.5916(2) | 0.28(1) |
| N(15) | -0.3520(2) | 0.6696(2) | -0.4036(2) | 0.26(1) |
| N(16) | -0.2591(2) | 0.4705(2) | -0.4457(2) | 0.36(1) |
| C(1) | -0.2615(2) | 0.8979(2) | -0.1186(2) | 0.23(1) |
| C(2) | -0.1019(2) | 0.8448(3) | -0.0209(2) | 0.26(1) |
| C(3) | -0.6216(3) | 1.2403(2) | -0.1047(2) | 0.24(1) |
| C(4) | -0.6612(3) | 1.4143(2) | -0.0115(2) | 0.25(1) |
| C(5) | -0.7871(2) | 1.0384(2) | -0.4684(2) | 0.24(1) |
| C(6) | -0.8995(2) | 1.1850(2) | -0.4928(2) | 0.26(1) |
| C(7) | -0.4347(2) | 0.7276(2) | -0.4695(2) | 0.23(1) |
| C(8) | -0.3353(2) | 0.5670(2) | -0.4822(2) | 0.25(1) |
| H(1) | -0.2481(35) | 0.7606(34) | -0.2413(32) | 0.40(10) |
| H(5) | -0.7413(35) | 1.2618(35) | -0.2391(33) | 0.44(10) |
| H(9) | -0.8641(37) | 0.9455(36) | -0.6357(34) | 0.51(11) |
| H(13) | -0.4959(32) | 0.6748(31) | -0.6440(30) | 0.33(8) |
| H(13A) | -0.8771(28) | 0.9026(35) | -0.2814(26) | 0.47(10) |
| H(13B) | -0.8339(41) | 0.9388(37) | -0.1612(25) | 0.67(13) |
| H(14A) | -0.3620(22) | 1.1411(45) | -0.3195(34) | 0.85(16) |
| H(14B) | -0.4646(35) | 1.0971(37) | -0.4206(17) | 0.57(11) |
| H(15A) | -0.5728(34) | 0.6258(24) | -0.2857(25) | 0.41(9) |
| H(15B) | -0.5539(50) | 0.6695(49) | -0.1680(27) | 0.94(17) |
| H(16A) | -0.5589(39) | 0.8414(43) | -0.0134(35) | 0.89(16) |
| H(16B) | -0.6511(39) | 0.9314(36) | -0.0061(31) | 0.76(14) |

Table 2
Bond distances (in nm)

| | | | |
|-------------|-----------|-------------|-----------|
| Pr–O(7) | 0.2378(2) | Pr–O(4) | 0.2394(2) |
| Pr–O(1) | 0.2405(2) | Pr–O(10) | 0.2457(2) |
| Pr–O(14) | 0.2499(2) | Pr–O(15) | 0.2549(2) |
| Pr–O(16) | 0.2573(2) | Pr–O(13) | 0.2608(2) |
| O(1)–C(1) | 0.1266(3) | O(2)–N(4) | 0.1232(3) |
| O(3)–N(4) | 0.1219(3) | O(4)–C(3) | 0.1267(3) |
| O(5)–N(8) | 0.1219(3) | O(6)–N(8) | 0.1215(3) |
| O(7)–C(5) | 0.1263(3) | O(8)–N(12) | 0.1220(3) |
| O(9)–N(12) | 0.1216(3) | O(10)–C(7) | 0.1261(3) |
| O(11)–N(16) | 0.1215(3) | O(12)–N(16) | 0.1225(4) |
| N(1)–C(1) | 0.1351(3) | N(1)–N(2) | 0.1358(3) |
| N(2)–C(2) | 0.1307(3) | N(3)–C(2) | 0.1343(3) |
| N(3)–C(1) | 0.1361(3) | N(4)–C(2) | 0.1436(3) |
| N(5)–C(3) | 0.1356(3) | N(5)–C(6) | 0.1369(3) |
| N(6)–C(4) | 0.1309(3) | N(7)–C(4) | 0.1341(3) |
| N(7)–C(3) | 0.1357(3) | N(8)–C(4) | 0.1452(3) |
| N(9)–N(10) | 0.1365(3) | N(9)–C(5) | 0.1366(3) |
| N(10)–C(6) | 0.1309(3) | N(11)–C(6) | 0.1336(3) |
| N(11)–C(5) | 0.1355(3) | N(12)–C(6) | 0.1449(3) |
| N(13)–N(14) | 0.1366(3) | N(13)–C(7) | 0.1373(3) |
| N(14)–C(8) | 0.1304(3) | N(15)–C(8) | 0.1335(3) |
| N(15)–C(7) | 0.1348(3) | N(16)–C(8) | 0.1451(3) |

and (IV) are 11.2°, 13.1°, 3.2°, 13.7°, 5.8° and 3.8°, respectively.

3.2. Mechanism of thermal decomposition of $\text{H}[\text{Pr}(\text{NTO})_4(\text{H}_2\text{O})_4]\cdot 2\text{H}_2\text{O}$

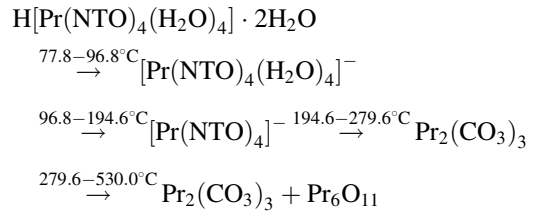
The DSC, DTA and TG curves for $\text{H}[\text{Pr}(\text{NTO})_4(\text{H}_2\text{O})_4]\cdot 2\text{H}_2\text{O}$ are shown in Fig. 4. The DSC curve shows that there are two endothermic and two exothermic processes at temperatures higher than 77.8°C. The first endothermic process is at 77.8–96.8°C, TG curve shows that the mass loss is 12.26% corresponding to this temperature range, which coincides with the calculated one, 4.70%, of losing two crystallization water molecules from the complex. The second endothermic process is at 96.8–194.6°C, the mass loss is 9.39%, which coincides with the calculated one, 9.40%, of losing four coordination water molecules. Further decomposition of the dehydrated complex would occur at 194.6–279.6°C, there is a rather severe mass loss (23.03%). The IR spectra of the residue at 300°C shows that the absorption peaks of $-\text{NO}_2$ disappear at 1513 and 1301 cm $^{-1}$ and the characteristic absorption peaks of $\text{Pr}_2(\text{CO}_3)_3$ appear at 1488 and 867 cm $^{-1}$. The last exothermic processes is at

Table 3
Bond angles (°)

| | | | |
|------------------|-----------|-------------------|-----------|
| O(7)–Pr–O(4) | 97.16(7) | O(7)–Pr–O(1) | 148.72(7) |
| O(4)–Pr–O(1) | 84.05(7) | O(7)–Pr–O(10) | 74.49(7) |
| O(4)–Pr–O(10) | 144.45(7) | O(1)–Pr–O(10) | 86.40(7) |
| O(7)–Pr–O(14) | 74.03(7) | O(4)–Pr–O(14) | 72.33(7) |
| O(1)–Pr–O(14) | 76.66(7) | O(10)–Pr–O(14) | 72.15(6) |
| O(7)–Pr–O(15) | 116.16(7) | O(4)–Pr–O(15) | 135.81(7) |
| O(1)–Pr–O(15) | 81.56(7) | O(10)–Pr–O(15) | 75.83(6) |
| O(14)–Pr–O(15) | 142.05(7) | O(7)–Pr–O(16) | 133.88(7) |
| O(4)–Pr–O(16) | 73.07(6) | O(1)–Pr–O(16) | 76.51(7) |
| O(10)–Pr–O(16) | 137.08(6) | O(14)–Pr–O(16) | 137.85(6) |
| O(15)–Pr–O(16) | 63.00(6) | O(7)–Pr–O(13) | 70.45(7) |
| O(4)–Pr–O(13) | 79.65(7) | O(1)–Pr–O(13) | 139.64(7) |
| O(10)–Pr–O(13) | 126.57(7) | O(14)–Pr–O(13) | 130.93(7) |
| O(15)–Pr–O(13) | 84.92(7) | O(16)–Pr–O(13) | 63.49(7) |
| C(1)–O(1)–Pr | 149.5(2) | C(3)–O(4)–Pr | 155.7(2) |
| C(5)–O(7)–Pr | 144.3(2) | C(7)–O(10)–Pr | 139.5(2) |
| C(1)–N(1)–N(2) | 111.6(2) | C(2)–N(2)–N(1) | 100.0(2) |
| C(2)–N(3)–C(1) | 100.9(2) | O(3)–N(4)–O(2) | 124.2(2) |
| O(3)–N(4)–C(2) | 118.3(2) | O(2)–N(4)–C(2) | 117.5(2) |
| C(3)–N(5)–N(6) | 110.9(2) | C(4)–N(6)–N(5) | 100.0(2) |
| C(4)–N(7)–C(3) | 101.0(2) | O(6)–N(8)–O(5) | 124.5(2) |
| O(6)–N(8)–C(4) | 118.0(2) | O(5)–N(8)–C(4) | 117.6(2) |
| N(10)–N(9)–C(5) | 111.5(2) | C(6)–N(10)–N(9) | 99.8(2) |
| C(6)–N(11)–C(5) | 101.8(2) | O(9)–N(12)–O(8) | 124.9(3) |
| O(9)–N(12)–C(6) | 118.4(3) | O(8)–N(12)–C(6) | 116.7(2) |
| N(14)–N(13)–C(7) | 111.2(2) | C(8)–N(14)–N(13) | 99.9(2) |
| C(8)–N(15)–C(7) | 102.2(2) | O(11)–N(16)–O(12) | 124.3(3) |
| O(11)–N(16)–C(8) | 118.5(3) | O(12)–N(16)–C(8) | 117.2(2) |
| O(1)–C(1)–N(1) | 125.3(2) | O(1)–C(1)–N(3) | 126.2(2) |
| N(1)–C(1)–N(3) | 108.5(2) | N(3)–C(2)–N(3) | 119.0(2) |
| N(2)–C(2)–N(4) | 119.4(2) | N(3)–C(2)–N(4) | 121.5(2) |
| O(4)–C(3)–N(5) | 125.1(2) | O(4)–C(3)–N(7) | 126.0(2) |
| N(5)–C(3)–N(7) | 108.9(2) | N(6)–C(4)–N(7) | 119.1(2) |
| N(6)–C(4)–N(8) | 119.2(2) | N(7)–C(4)–N(8) | 121.7(2) |
| O(7)–C(5)–N(11) | 128.5(2) | O(7)–C(5)–N(9) | 123.7(2) |
| N(11)–C(5)–N(9) | 107.8(2) | N(10)–C(6)–N(11) | 119.1(2) |
| N(10)–C(6)–N(12) | 119.4(2) | N(11)–C(6)–N(12) | 121.5(2) |
| O(10)–C(7)–N(15) | 127.8(2) | O(10)–C(7)–N(13) | 124.6(2) |
| N(15)–C(7)–N(13) | 107.5(2) | N(14)–C(8)–N(15) | 119.0(2) |
| N(14)–C(8)–N(16) | 120.0(2) | N(15)–C(8)–N(16) | 120.8(2) |

279.6–530.0°C, and the mass loss is 18.21%. The IR spectra of the residue at 550°C shows that there is the weaker absorption of $\text{Pr}_2(\text{CO}_3)_3$ at 1488 and 867 cm^{-1} and the absorption peak of Pr_6O_{11} forms at 402 cm^{-1} .

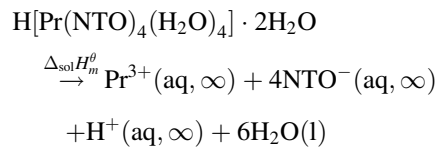
On the bases of experimental and calculated results, the thermal decomposition mechanism of $\text{H}[\text{Pr}(\text{NTO})_4(\text{H}_2\text{O})_4]\cdot 2\text{H}_2\text{O}$ is postulated to be as follows:



3.3. Enthalpy of solution in water of $\text{H}[\text{Pr}(\text{NTO})_4(\text{H}_2\text{O})_4]\cdot 2\text{H}_2\text{O}$

The mean of the enthalpy of solution of $\text{H}[\text{Pr}(\text{NTO})_4(\text{H}_2\text{O})_4]\cdot 2\text{H}_2\text{O}$ in deionized water at 298.15 K is $87.45 \pm 0.49 \text{ kJ mol}^{-1}$. The molar ratio $n(\text{H}_2\text{O})/n\{\text{H}[\text{Pr}(\text{NTO})_4(\text{H}_2\text{O})_4]\cdot 2\text{H}_2\text{O}\}$ are 47 000–83 405. Therefore, the mean of $\Delta_{\text{sol}}H_m^\theta$ can be considered at infinite dilution.

Because $\text{H}[\text{Pr}(\text{NTO})_4(\text{H}_2\text{O})_4]\cdot 2\text{H}_2\text{O}$ is completely ionized in aqueous solution, its ionization process can be represented as



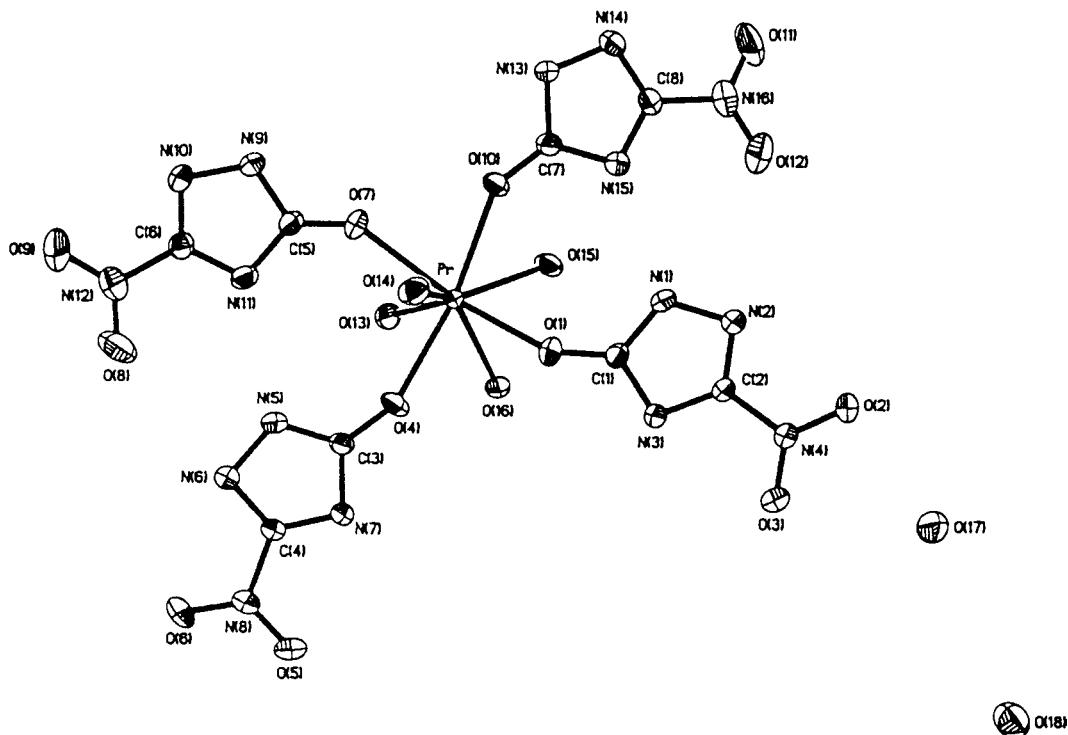
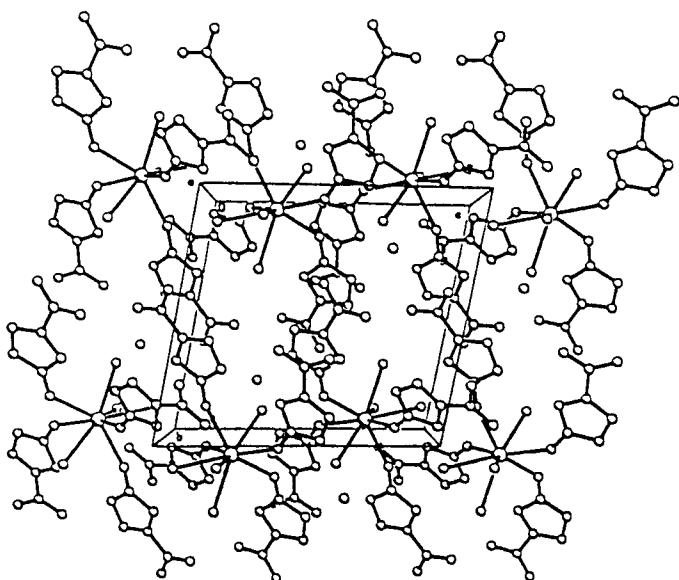
3.4. Standard enthalpy of formation of $\text{H}[\text{Pr}(\text{NTO})_4(\text{H}_2\text{O})_4]\cdot 2\text{H}_2\text{O}$, $\Delta_fH_m^\theta\{\text{H}[\text{Pr}(\text{NTO})_4(\text{H}_2\text{O})_4]\cdot 2\text{H}_2\text{O}, \text{cr}, 298.15 \text{ K}\}$

By substituting the mean of $\Delta_{\text{sol}}H_m^\theta$ and the reported values of $\Delta_fH_m^\theta(\text{Pr}^{3+}, \text{aq}, \infty) = -704.47 \text{ kJ mol}^{-1}$ [8]; $\Delta_fH_m^\theta(\text{NTO}^-, \text{aq}, \infty) = -(94.3 \pm 2.1) \text{ kJ mol}^{-1}$ [9]; $\Delta_fH_m^\theta(\text{H}^+, \text{aq}, \infty) = 0$ [8]; $\Delta_fH_m^\theta(\text{H}_2\text{O, l}) = -285.83 \text{ kJ mol}^{-1}$ [10], into Eq. (2),

$$\begin{aligned} & \Delta_fH_m^\theta\{\text{H}[\text{Pr}(\text{NTO})_4(\text{H}_2\text{O})_4] \cdot 2\text{H}_2\text{O, cr, 298.15 K}\} \\ & = \Delta_fH_m^\theta(\text{Pr}^{3+}, \text{aq}, \infty) \\ & \quad + 4\Delta_fH_m^\theta(\text{NTO}^-, \text{aq}, \infty) \\ & \quad + \Delta_fH_m^\theta(\text{H}^+, \text{aq}, \infty) + 6\Delta_fH_m^\theta(\text{H}_2\text{O, l}) \\ & \quad - \Delta_{\text{sol}}H_m^\theta \end{aligned} \quad (2)$$

the following value was obtained:

$$\begin{aligned} & \Delta_fH_m^\theta\{\text{H}[\text{Pr}(\text{NTO})_4(\text{H}_2\text{O})_4] \cdot 2\text{H}_2\text{O, cr, 298.15 K}\} \\ & = -(2884.1 \pm 8.9) \text{ kJ mol}^{-1} \end{aligned}$$

Fig. 1. Molecular structure of $\text{H}[\text{Pr}(\text{NTO})_4(\text{H}_2\text{O})_4]\cdot 2\text{H}_2\text{O}$.Fig. 2. Packing of the molecule $\text{H}[\text{Pr}(\text{NTO})_4(\text{H}_2\text{O})_4]\cdot 2\text{H}_2\text{O}$ in the crystal lattice.

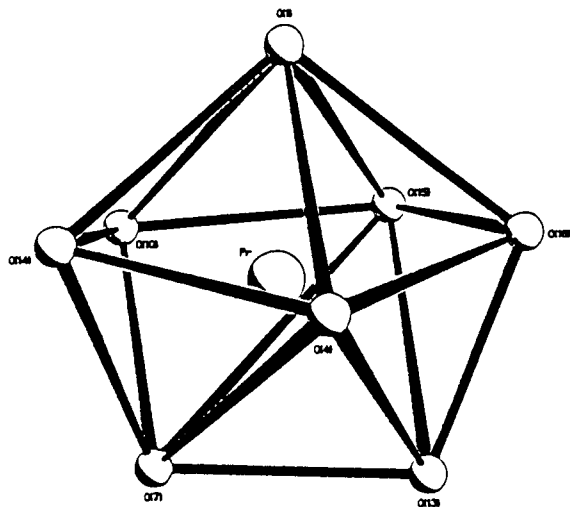
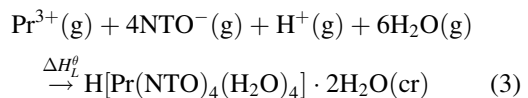


Fig. 3. Coordination polyhedron of Pr^{3+} in $\text{H}[\text{Pr}(\text{NTO})_4 \cdot (\text{H}_2\text{O})_4] \cdot 2\text{H}_2\text{O}$.

3.5. Lattice enthalpy and energy of $\text{H}[\text{Pr}(\text{NTO})_4 \cdot (\text{H}_2\text{O})_4] \cdot 2\text{H}_2\text{O}$, $\Delta H_L^\theta \{ \text{H}[\text{Pr}(\text{NTO})_4 \cdot (\text{H}_2\text{O})_4] \cdot 2\text{H}_2\text{O}, \text{cr} \}$, $\Delta U_L^\theta \{ \text{H}[\text{Pr}(\text{NTO})_4 \cdot (\text{H}_2\text{O})_4] \cdot 2\text{H}_2\text{O}, \text{cr} \}$

Setting $\Delta H_L^\theta \{ \text{H}[\text{Pr}(\text{NTO})_4 \cdot (\text{H}_2\text{O})_4] \cdot 2\text{H}_2\text{O}, \text{cr} \}$ as the lattice enthalpy in forming the crystal $\text{H}[\text{Pr}(\text{NTO})_4 \cdot (\text{H}_2\text{O})_4] \cdot 2\text{H}_2\text{O}$ from $\text{Pr}^{3+}(\text{g})$, $\text{NTO}^-(\text{g})$, $\text{H}^+(\text{g})$ and

$\text{H}_2\text{O}(\text{g})$ at 298.15 K, and $\Delta U_L^\theta \{ \text{H}[\text{Pr}(\text{NTO})_4 \cdot (\text{H}_2\text{O})_4] \cdot 2\text{H}_2\text{O}, \text{cr} \}$ as the crystal lattice energy



we have

$$\begin{aligned} & \Delta H_L^\theta \{ \text{H}[\text{Pr}(\text{NTO})_4 \cdot (\text{H}_2\text{O})_4] \cdot 2\text{H}_2\text{O}, \text{cr} \} \\ & = \Delta_f H_m^\theta \{ \text{H}[\text{Pr}(\text{NTO})_4 \cdot (\text{H}_2\text{O})_4] \cdot 2\text{H}_2\text{O}, \text{cr}, 298.15 \text{ K} \} - \Delta_f H_m^\theta (\text{Pr}^{3+}, \text{g}) \\ & - 4\Delta_f H_m^\theta (\text{NTO}^-, \text{g}) - \Delta_f H_m^\theta (\text{H}^+, \text{g}) \\ & - 6\Delta_f H_m^\theta (\text{H}_2\text{O}, \text{g}) \end{aligned} \quad (4)$$

and

$$\begin{aligned} & \Delta U_L^\theta \{ \text{H}[\text{Pr}(\text{NTO})_4 \cdot (\text{H}_2\text{O})_4] \cdot 2\text{H}_2\text{O}, \text{cr} \} \\ & = \Delta H_L^\theta \{ \text{H}[\text{Pr}(\text{NTO})_4 \cdot (\text{H}_2\text{O})_4] \cdot 2\text{H}_2\text{O}, \text{cr} \} \\ & - \Delta n R T, \end{aligned} \quad (5)$$

where $\Delta_f H_m^\theta (\text{Pr}^{3+}, \text{g}) = 4001.33 \text{ kJ mol}^{-1}$ [8]; $\Delta_f H_m^\theta (\text{NTO}^-, \text{g}) = -374.3 \text{ kJ mol}^{-1}$ [11]; $\Delta_f H_m^\theta (\text{H}^+, \text{g}) = 1535.94 \text{ kJ mol}^{-1}$ [8]; $\Delta_f H_m^\theta (\text{H}_2\text{O}, \text{g}) = -241.82 \text{ kJ mol}^{-1}$ [10]; $\Delta n = -12$; $R T = 2.5 \text{ kJ mol}^{-1}$.

By substituting the above-mentioned data into Eqs. (4) and (5), the following values are obtained:

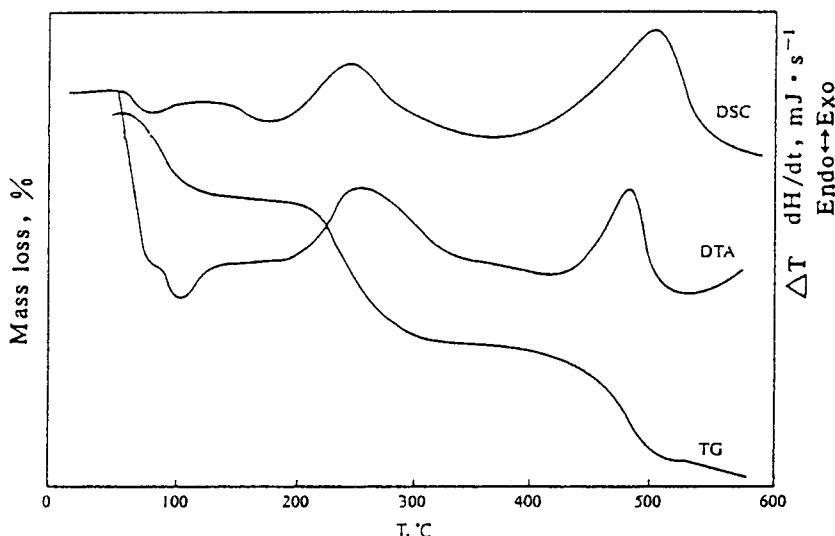


Fig. 4. DSC, DTA and TG curves for $\text{H}[\text{Pr}(\text{NTO})_4 \cdot (\text{H}_2\text{O})_4] \cdot 2\text{H}_2\text{O}$ at a heating rate of $10^\circ\text{C min}^{-1}$.

$$\Delta H_L^\theta \{ \text{H}[\text{Pr}(\text{NTO})_4(\text{H}_2\text{O})_4] \cdot 2\text{H}_2\text{O, cr} \} \\ = -5473.25 \text{ kJ mol}^{-1};$$

$$\Delta U_L^\theta \{ \text{H}[\text{Pr}(\text{NTO})_4(\text{H}_2\text{O})_4] \cdot 2\text{H}_2\text{O, cr} \} \\ = -5443.25 \text{ kJ mol}^{-1}.$$

References

- [1] K.Y. Lee, L.B. Chapman, M.D. Coburn, J. Energetic Mater. 5 (1987) 27.
- [2] E.F. Rothenberg, D.E. Audette, R.C. Wedlich, Thermochim. Acta 185 (1991) 235.
- [3] Song Jirong, Hu Rongzu, Li Fuping, Chinese Science Bulletin 41(21) (1996) 1806.
- [4] Song Jirong, Chen Zhaoxu, Xiao Heming, Hu Rongzu, Li Fuping, Acta Chimica Sinica 56(3) (1998) 270.
- [5] Hu Rongzu, Song Jirong, Li Fuping, Thermochimica Acta 229 (1997) 87.
- [6] Song Jirong, Dong Wu, Hu Rongzu, J. Rare Earths 15(1) (1997) 62.
- [7] R.C. Weast, CRC Handbook of Chemistry and Physics, 70th ed., CRC Press, Boca Raton, Florida, 1989, D-122.
- [8] R.C. Weast, CRC Handbook of Chemistry and Physics, 63rd ed., CRC Press, Boca Raton, Florida, 1982–1983, D-82, D-71.
- [9] A. Finch, P.J. Gardner, A.J. Head, H.S. Majdi, J. Chem. Thermodyn. 23(12) (1991) 1169.
- [10] R.C. Weast, CRC Handbook of Chemistry and Physics, 58th ed., CRC Press, Boca Raton, Florida, 1977–1978, D-85.
- [11] Hu Rongzu, Meng Zihui, Kang Bing, Thermochim. Acta 275 (1996) 159.